Twentieth-Century Drought in the Conterminous United States

KONSTANTINOS M. ANDREADIS, ELIZABETH A. CLARK, ANDREW W. WOOD, ALAN F. HAMLET, AND DENNIS P. LETTENMAIER

Department of Civil and Environmental Engineering, University of Washington, Seattle, Washington

(Manuscript received 18 November 2004, in final form 20 April 2005)

ABSTRACT

Droughts can be characterized by their severity, frequency and duration, and areal extent. Depth–area–duration analysis, widely used to characterize precipitation extremes, provides a basis for the evaluation of drought severity when storm depth is replaced by an appropriate measure of drought severity. Gridded precipitation and temperature data were used to force a physically based macroscale hydrologic model at 1/2° spatial resolution over the continental United States, and construct a drought history from 1920 to 2003 based on the model-simulated soil moisture and runoff. A clustering algorithm was used to identify individual drought events and their spatial extent from monthly summaries of the simulated data. A series of severity–area–duration (SAD) curves were constructed to relate the area of each drought to its severity. An envelope of the most severe drought events in terms of their SAD characteristics was then constructed. The results show that (a) the droughts of the 1930s and 1950s were the most severe of the twentieth century for large areas; (b) the early 2000s drought in the western United States is among the most severe in the period of record, especially for small areas and short durations; (c) the most severe agricultural droughts were also among the most severe hydrologic droughts, however, the early 2000s western U.S. drought occupies a larger portion of the hydrologic drought envelope curve than does its agricultural companion; and (d) runoff tends to recover in response to precipitation more quickly than soil moisture, so the severity of hydrologic drought during the 1930s and 1950s was dampened by short wet spells, while the severity of the early 2000s drought remained high because of the relative absence of these short-term phenomena.

1. Introduction

Drought is among the most costly of the natural disasters. In 1995, the U.S. Federal Emergency Management Agency (Federal Emergency Management Agency 1995) estimated that the annual cost of U.S. droughts was in the range of $6–$8 billion. According to the National Oceanic and Atmospheric Administration's (NOAA's) National Climate Data Center (2003; NCDC), the 1988 drought alone cost nearly $62 billion (in 2002 dollars), making it the most costly natural disaster in U.S. history. Webb et al. (2004) suggest that the recent western U.S. drought could be the most severe in the last 500 yr, based on tree-ring analysis. Dai et al. (2004) report a tendency toward more extreme droughts over the past two to three decades resulting from global warming. Furthermore, the drying of soils associated with this warming enhances the risk of long-duration droughts.

To assess the potential impacts of drought, water managers often compare current or potential drought severity for a given location (or river basin) with the severity of historical droughts. However, this approach overlooks the effects of areal extent on drought intensity. The potential for costly and widespread drought conditions argues for the development of more comprehensive methods for drought characterization.

The overall impact of a drought depends on several factors, including not only its severity, but also frequency, area, and duration. Several drought indices have been defined (primarily for the characterization of drought severity), which typically describe one of the following four drought types: agricultural, hydrologic, meteorological, and socioeconomic. Generally, agricultural drought is related to soil moisture, hydrologic drought to runoff and streamflow, meteorological drought to precipitation, and socioeconomic drought to the disparity between the supply and demand for water (Wilhite and Glantz 1985). This paper focuses on agri-

Corresponding author address: Dennis P. Lettenmaier, Department of Civil and Environmental Engineering, University of Washington, Box 352700, Seattle, WA 98195.
E-mail: dennisl@u.washington.edu

© 2005 American Meteorological Society

Unauthenticated | Downloaded 08/22/22 08:12 PM UTC

cultural and hydrologic drought over the continental United States.

For long-term drought characterization, the Palmer Drought Severity Index (PDSI; Palmer 1965) is the most widely used drought index. PDSI is a measure of meteorological drought; however, the method accounts for evapotranspiration and soil moisture conditions, as well as precipitation, both of which are determinants of hydrologic drought (Alley 1984); therefore, it is related to hydrologic (and agricultural) drought as well. Dai et al. (2004) report correlations between annual PDSI and streamflow globally. They also find a positive correlation between PDSI and soil moisture during warm seasons at a regional or river-basin scale, although they note that PDSI should not be used as a measure of soil moisture in cold seasons or at high latitudes because snow interferes with soil moisture calculations in PDSI. For these (and other) reasons, PDSI is generally considered to be inadequate for characterization of agricultural or hydrologic drought.

Nonetheless, the attraction to PDSI is its standardization, which theoretically should enable comparisons of drought intensity across heterogeneous regions. Palmer (1965) provides a clear indication of how the initialization and termination of drought can be estimated using PDSI. However, PDSI values are highly sensitive to termination criteria, which are somewhat arbitrary (Alley 1984). As a result, spatial patterns of PDSI sometimes defy physical explanation, with some areas commonly experiencing severe droughts and others rarely experiencing drought (Willeke et al. 1994) despite climate conditions that would suggest otherwise. Although other drought indicators, such as soil moisture in the case of agricultural drought or runoff as a measure of hydrologic drought, reflect an adequate physical basis for interpretation, they are often constrained by data availability.

Soulé (1993) notes that when analyzing drought trends, finescale data should be used to account for the spatial heterogeneity of drought patterns. Because stream gauges integrate over relatively large spatial areas (especially in the case of the relatively small number of gauges that have been operated continuously for a half-century or more), and because stream gauges are often located to benefit water resources operations, they do not generally resolve spatial variability of hydrologic drought adequately. Long-term soil moisture data (i.e., records longer than a few decades) are virtually nonexistent in the United States (except in Illinois and Iowa; Robock et al. 2000); hence, direct estimation of long-term statistics of agricultural drought for the continental United States is essentially impossible. These factors are a major reason for the widespread use of PDSI, despite its known shortcomings. A standard approach to mapping drought is to assign a single PDSI value, based on station data, to each of 344 climatic divisions of the contiguous United States (e.g., Soulé 1993). Alternately, several studies have interpolated tree-ring chronologies to produce gridded PDSI datasets, thereby extending the record of drought to as far back as 1700 (Karl and Koscielny 1982; Cook et al. 1999).

An alternative to these methods is to use physically based hydrologic models to simulate variables (soil moisture, runoff) from which agricultural and hydrologic drought can be computed using consistent gridded datasets of the model meteorological forcings. The output of these models can be used to map the spatial extent of drought. NOAA's Climate Prediction Center (2005; CPC), for example, estimates soil moisture, evaporation, and runoff from observed temperature and precipitation using a one-layer hydrological model (Huang et al. 1996). Although spatially contiguous datasets of relevant parameters have been developed, relationships between the area of an individual drought event and its severity have not been fully explored.

The U.S. Drought Monitor (2003) produces maps of drought extent and severity using a combination of several drought indicators, including PDSI, CPC-simulated soil moisture (percentiles), U.S. Geological Survey weekly observed streamflow (percentiles), standardized precipitation index, and a satellite vegetation health index. The weighting of these indicators combines objective and subjective characterization techniques to reflect conditions in various regions and at different times of the year. CPC is also experimenting with more objective blends of drought indicators as a supplemental tool.

Following the CPC, we employ a macroscale hydrologic model to simulate soil moisture and runoff for the conterminous United States. Rather than use climate division data, we perform a retrospective analysis of historical droughts from 1920 through 2003 using recently released digitized Cooperative Observer Network (Coop) station data from NOAA's NCDC, which we grid to 1/2° spatial resolution. For simplicity, and to maintain objectivity in the weighting of factors, we use soil moisture percentile anomalies as an indicator of agricultural drought severity. The relative severity of agricultural droughts is then compared with that of hydrologic drought as designated by runoff percentile anomalies.

The purpose of this study is to identify the major drought events of the twentieth century in the continental Unites States based not only on their severity, but also on their areal extent and duration. Several

Unauthenticated | Downloaded 08/22/22 08:12 PM UTC

studies have used principal component analysis of gridded PDSI, derived from historical climate data, to delineate spatially homogeneous areas of drought and to relate these to global-scale climate patterns, such as El Niño–Southern Oscillation (ENSO) or the Pacific Decadal Oscillation (PDO) (e.g., Karl and Koscielny 1982; Dai et al. 1998; Dai et al. 2004; Schubert et al. 2004). Fewer studies have examined the relative extent of individual drought events or the relationship between drought severity and areal extent. Sheffield et al. (2004) have evaluated drought severity and extent using a macroscale simulation model output similar to ours, but with somewhat different analytical methods.

Others have used historical drought records to relate drought severity to duration and frequency. Dalezios et al. (2000) developed a severity–duration–frequency analysis, using PDSI data for 1957–83, based on intensity–duration–frequency relationships that are typically used to synthesize design storms. We adapt another tool that is typically used to characterize storm precipitation: depth–area–duration (DAD) analysis (World Meteorological Organization 1969). For drought analysis, we simply replace depth of precipitation with a measure of drought severity. In so doing, we take advantage of the high-resolution spatial data, simulated by a physically based hydrologic model, to include area in our definition of drought intensity. We will refer to this technique as severity–area–duration (SAD) analysis.

2. Dataset description

The recent availability of Cooperative Observer station meteorological daily data (DSI-3206) for the pre-1949 period enabled extension of our analysis from the 1950–2000 period used by Sheffield et al. (2004) [based, in turn, on the derived hydrologic data archive for the continental United States described by Maurer et al. (2002)] to encompass the early twentieth century as well. The NCDC now maintains electronic archives of digitized versions of all data provided by its Cooperative Observers within the 50 states, as well as in Puerto Rico and the U.S. Virgin Islands. We merged these data with a previously released cooperative station dataset (DSI-3200) to create a continuous record for the 1915–2003 period. Like DSI-3200, DSI-3206 includes air temperature with observation times at 7 A.M., 2 P.M., and 9 P.M.; daily maximum, minimum, and mean temperatures; total precipitation, snowfall, and depth of snow on the ground; prevailing wind direction and total wind movement; evaporation; sky condition; and occurrence of weather and obstructions to vision (National Climatic Data Center 2003); although the data density for precipitation and air temperature maxima and minima is generally much higher than for the other variables. We gridded data from 2489 stations for precipitation and 1904 stations for temperature to 1/2° spatial resolution using the methods outlined in Maurer et al. (2002), then aggregated the data to over the North American Land Data Assimilation System (NLDAS) domain, which includes all of North America from 25° to 53°N latitude (Mitchell et al. 2004).

We applied methods described in Hamlet and Lettenmaier (2005) to correct for temporal heterogeneities in the data. This method essentially adjusts the gridded data to have decadal-scale variability that is comparable to that of the U.S. Historical Climatology Network (HCN) in the United States [and the Historical Canadian Climate Database (HCCD) in Canada]. HCN (Karl et al. 1990) and HCCD (Mekis and Hogg 1999; Vincent and Gullett 1999) are high-quality station datasets that have been carefully adjusted for effects of changes in instrumentation and other factors that are not related to natural climate variability over the period of record. The resultant adjusted dataset reproduces the monthly precipitation and temperature trends of the HCN and HCCD data, while retaining the spatial information from the larger number of stations in the Coop records. The final forcing dataset also includes a topographical precipitation correction, described in Maurer et al. (2002), based on the Precipitation Regression on Independent Slopes Method (PRISM) precipitation maps (Daly et al. 1994).

3. Hydrology model description

We used the Variable Infiltration Capacity (VIC) model (Liang et al. 1994, 1996; Cherkauer and Lettenmaier 2003) to simulate historical soil moisture and runoff over the NLDAS domain. The VIC model balances energy and moisture fluxes over each grid cell (1/2° latitude × 1/2° longitude in this case). The model includes a soil–vegetation–atmosphere transfer (SVAT) scheme, which represents the controls exerted by vegetation and soil moisture on land–atmosphere moisture and energy fluxes. VIC accounts for the effects of subgrid-scale variability in soil, vegetation, precipitation, and topography on grid-scale fluxes. It represents the subsurface as three layers—a relatively thin surface layer, from which surface or "fast" runoff is generated, and two progressively deeper layers, which control subsurface runoff generation. In this study, we used the same soils, vegetation, and topographic data as in Maurer et al. (2002), aggregated to the 1/2° spatial resolution. The Maurer et al. data are, in turn, quite similar to those used in NLDAS (Mitchell et al. 2004).

Several studies have successfully simulated runoff

Unauthenticated | Downloaded 08/22/22 08:12 PM UTC

and streamflow using the VIC model over large river basins and at continental to global scales for multidecadal periods (e.g., Abdulla et al. 1996; Lohmann et al. 1998; Nijssen et al. 1997, 2001; Wood et al. 1997; Maurer et al. 2002). Nijssen et al. (2001) report good correspondence between the annual cycle and spatial patterns of soil moisture that are simulated by VIC and the observed soil moisture in central Illinois and central Eurasia. Likewise, Maurer et al. (2002) find that observed soil moisture persistence is better represented by the VIC model than the Huang et al. (1996) model, which is used by the U.S. Drought Monitor. They also note that over shorter time scales, VIC-derived soil moisture is well suited for use in diagnostic studies. Furthermore, Robock et al. (2003) showed good agreement of spatially averaged soil moisture between VIC and Mesonet stations over the Southern Great Plains, although VIC underestimated the seasonal variation of soil moisture.

For this study, the period for which simulations were performed was January 1915 through December 2003, using a daily time step in the water balance mode (which means that the surface temperature was set to surface air temperature, rather than being iterated for energy balance closure). As in Maurer et al. (2002), soil depths varied from 0.1 to 0.5 m for the upper layer, from 0.2 to 2.4 m for the middle layer, and from 0.1 to 2.5 m for the lower layer. Exploratory analysis indicated that as much as a decade is necessary to fully remove the effects of initial soil moisture conditions, especially in dry regions. To minimize the spinup period, we averaged January soil moisture values (to coincide with the starting date of our simulations) from an uninitialized simulation for the period of 1925–2003 and took these as initial soil moisture for subsequent runs. Exploratory analyses have suggested that the soil moisture equilibration time required for VIC ranges from 6 months (Cosgrove et al. 2003) to a decade. Therefore, we used the period of 1915–19 for spinup, and performed our analysis for the period of 1920–2003.

4. Soil moisture and runoff percentiles

One approach to defining drought severity is to measure the degree of departure from normal. In this paper, we use soil moisture anomalies as a measure of agricultural drought and runoff anomalies as a measure of hydrologic drought. Our desire is to develop a method that allows direct comparison of droughts across the domain. Use of absolute magnitude (e.g., of soil moisture deficits) is not appropriate for this purpose because anomalies in absolute terms reflect different severities in different parts of the domain. The use of percentiles, which by construct have a range from zero to one (and are uniformly distributed over this range), is more appropriate for our purposes.

Monthly percentiles were calculated for each grid cell based on the climatology of the 84-yr study period. Soil moisture in each of the three soil layers was accumulated for each month to produce a single value of total column soil moisture. Empirical cumulative probability distributions were formed for each grid cell and each month for soil moisture and runoff (using the Weibull plotting position), and the raw total column soil moisture and runoff were replaced by their percentiles.

5. Drought identification in space and time

Fundamental descriptors of droughts include their intensity and duration (Dracup et al. 1980b). Duration can be defined as the number of consecutive time steps that the time series (of soil moisture or runoff) is below a specified threshold level (Byun and Wilhite 1999), intensity is defined as the averaged cumulative departure from the threshold level for that duration, while severity is defined as the product of intensity and duration (cumulative departure from the drought threshold). Because droughts are regional phenomena that can cover large areas for long periods of time, the spatial extent of a drought is an equally important feature. Most previous studies have focused their analysis of the spatial patterns of drought on readily available point data (Soulé 1993). Statistical methods, such as correlation analysis (Oladipo 1986) and empirical orthogonal functions (EOFs), have been used (Dai et al. 1998, 2004; Cook et al. 1999; Hisdal and Tallaksen 2003) to estimate the regional characteristics of droughts as estimated from point or gridded data. These methods group stations that exhibit similar behavior in a statistical sense, for regionalization purposes. In this paper, we instead exploit the areal estimates of hydrologic variables that are provided by VIC simulations to evaluate drought extent. Our simulations provide spatially and temporally continuous mapping of (transformed) soil moisture and runoff over our domain, and it is, therefore, possible to evaluate spatial patterns of drought directly from the derived data, using the methods outlined below.

An objective definition of drought events is elusive, and many have been given depending on the context of the application. One of the most widely used methods for drought classification is based on defining a threshold level below which a drought is said to have occurred (Dracup et al. 1980a). An important aspect of this method is the selection of the threshold (or truncation) value. The PDSI, for example, is highly sensitive to

Unauthenticated | Downloaded 08/22/22 08:12 PM UTC

termination criteria (Alley 1984). A relatively high moisture threshold, such as the mean of a streamflow time series, would result in a large number of drought events. Given the temporal and spatial dimensions of the study domain, it is more appropriate to focus on moderate to extreme droughts. The CPC classifies droughts based on simulated soil moisture percentiles (from a 70-yr record of 1931–2000), among other indicators, and uses the following classification scheme: moderate drought (11%–20%), severe drought (6%–10%), extreme drought (3%–5%), and exceptional drought (0%–2%) (U.S. Drought Monitor 2003; Climate Prediction Center 2005). Following this scheme, we define the beginning and end of drought conditions based on a soil moisture (or runoff) percentile value of 20%.

The spatial identification procedure is based on a simple clustering algorithm that incorporates spatial contiguity. The process involves the initial partitioning of the data for each month of the time series into a number of clusters, and the subsequent merging of those based on minimum area constraints. Because droughts are regional phenomena, it can be argued that the prominent spatial characteristic of a drought event is the contiguity of its extent. Consequently, the distance between pixels that are under drought should facilitate the regionalization procedure.

The algorithm begins with a spatial smoothing preprocessing step. The spatial filter selected is a 3×3 median filter, which ensures minimum distortion of the original data. At each monthly time step, all pixels that have a soil moisture (or runoff) percentile value below 20% are considered as being "under drought." Those pixels are then classified into drought classes using a simple clustering algorithm. The first pixel under drought is assigned to the first class. Then, the 3×3 neighborhood of this pixel is searched for pixels under drought that are classified in the same drought cluster. This procedure is repeated until no pixels in the 3×3 neighborhood of the current pixel are under drought, and a new cluster is created for the next pixel below the drought threshold. After the initial partitioning step, the final classification step is to apply a minimum area threshold to each cluster (taken here as 10 pixels). If a cluster contains less than 10 pixels, it is not included in any of the subsequent calculations. At the end of this step, the remaining clusters are defined as separate drought events for the current time step.

Using this procedure, drought events are allowed to have variable duration and spatial extent, and are not confined to a predefined climate region. Therefore, we have to take into account the cases when multiple clusters merge to form a larger drought in later time steps, or a drought event breaks up into multiple smaller droughts. In both cases, the smaller droughts are considered to be part of the larger drought, but their spatial extents and severities are calculated separately by imposing a contiguity constraint. This is demonstrated in Fig. 1, which shows how the algorithm classifies two drought events for three consecutive time steps. In time step 1 (Fig. 1a), there are four drought events. The two droughts in the western United States, however, merge into one spatially larger event in time step 2 (Fig. 1b), which also occupies the same area over the next time step. Obviously the two drought areas (A1 and A2) in time step 1 should be considered as belonging to the same drought event. On the other hand, the drought area covering the southeastern United States in time

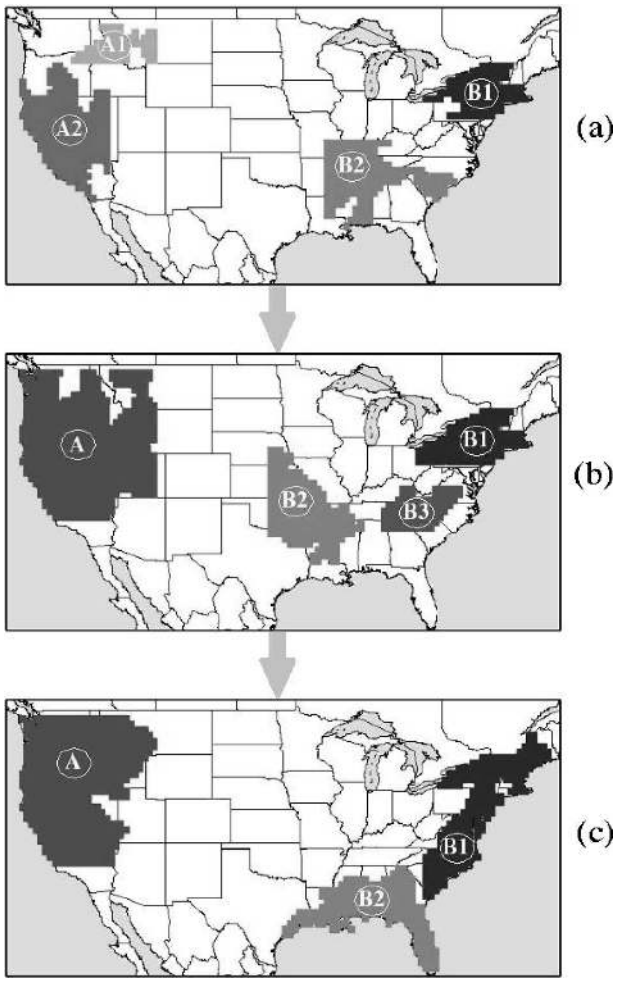

FIG. 1. Spatiotemporal drought identification: (a)–(c) three consecutive time steps, with two drought areas merging (A1 and A2), and drought area B2 breaking up into two drought areas, B2 and B3, with the latter merging with another drought area (B1). The algorithm classifies each smaller drought area to a larger drought event (A and B, respectively).

Unauthenticated | Downloaded 08/22/22 08:12 PM UTC

step 1 breaks off into two subdroughts in time step 2 (B2 and B3). These areas are classified in the same larger drought event, but their corresponding severities are computed separately for the time steps during which they are not spatially contiguous. In time step 3 (Fig. 1c), one of the drought areas that broke off merges with the drought over the northeastern region. Our approach is to reclassify all of these areas as belonging to the same larger event, on the basis that the driving climatic variables are the same.

6. Construction of drought severity–area–duration curves

DAD relationships of precipitation are used in engineering studies to estimate an areal reduction factor (ARF) for the reduction of point to areal precipitation (Grebner and Roesch 1997). This areal precipitation is then used in runoff volume computations to determine design storms for the design of small flood control structures (Dhar and Nandargi 1993). Just as depths of precipitation characterize extreme wet events, deficits of moisture characterize extreme dry events. Based on the distribution of these deficits in time and space, we can also characterize drought using its areal extent and duration. Therefore, we translate the DAD approach to evaluate drought conditions by replacing depth with a measure of severity. For the purposes of this paper, severity (S) is defined as $S = (1 - \Sigma P/t)*100\%$, where ΣP is the monthly percentile of soil moisture or runoff summed over duration t (with t in months). Because model output is gridded, we do not need to construct isohyetal maps, as is done in the classical DAD analysis of storms. Instead, we adapted the computational method of the World Meteorological Organization (1969) to calculate the average severity corresponding to each standard area. For this study, we examine durations of 3, 6, 9, 12, 24, 36, 48, and 72 months, and areas from 10 grid cells, or approximately 25 000 km^2, to the maximum drought extent of about 10^6 km^2, in increments of 20 grid cells, or approximately 50 000 km^2.

The process that is used to calculate drought severity at each duration starts with the grid cells being ranked by severity. Those cells with the maximum severity are used as potential "drought centers," corresponding to the storm centers of DAD analysis. The 3×3 neighborhood of the first drought center is identified, and the area of the neighboring cell with the highest severity is added to that of the first. Their severities are averaged, and the two cells collectively form an intermediate drought area. Then, the cells neighboring this intermediate drought area are identified, and the area of the cell with the maximum severity is added to the intermediate drought area. Once the first standardized area is reached, the severity and area are recorded. The process continues until all cells areas under drought are summed and the severities are averaged.

Because the area surrounding the first drought center might not match the maximum severity for a given area interval, we repeat this procedure on each of the remaining drought centers. For each duration, the combination of concurrent months that experienced the highest severity provides the severity for its corresponding area interval. The resultant plots reflect a drought-centered, absolute SAD relationship, which can be used to estimate absolute drought magnitudes without being constrained to an individual basin or area (see Grebner and Roesch 1997).

After calculating SAD relationships for each drought event, we identify the maximum severity events for each area interval and duration. These are used to generalize an enveloping relationship of the most extreme drought events in the United States between 1920 and 2003.

7. Results

a. Soil moisture droughts

Based on the drought threshold that is selected for the soil moisture–based analysis (20%), and the drought definition used in this study, 248 drought events were identified over the simulation period (1920–2003). However, only four of these spanned the maximum duration of our analysis (72 months), while most lasted for less than 6 months (189 events). The longest droughts occurred during the 1930s (1932–38), 1950s (1950–57), 1960s (1960–67), and late 1980s (1987–93); each of these had a duration of 6–7 yr. Other notably long events occurred in 1975–79, 1958–62, 1998–2003, and 1928–32. With respect to spatial extent, the drought events that stand out occurred during the 1930s and 1950s and covered almost the entire continental United States. Not surprisingly, other spatially expansive events coincided with the longest duration events, but with differences in the relative order. In terms of spatial extent, they ranked, from largest to smallest, as follows: 1987–93, 1998–2003, 1960–67, 1975–79, 1928–32, and 1938–41.

The spatial patterns of each of the major agricultural droughts identified (using soil moisture) are shown in Fig. 2, as the monthly soil moisture–derived drought severity for the four major drought events. The months shown were selected based on the average severity of each pixel in the drought times the pixel area. It is clear from these maps that the 1930s, 1950s, and 1988 droughts were the most extensive events in the twenti-

Unauthenticated | Downloaded 08/22/22 08:12 PM UTC

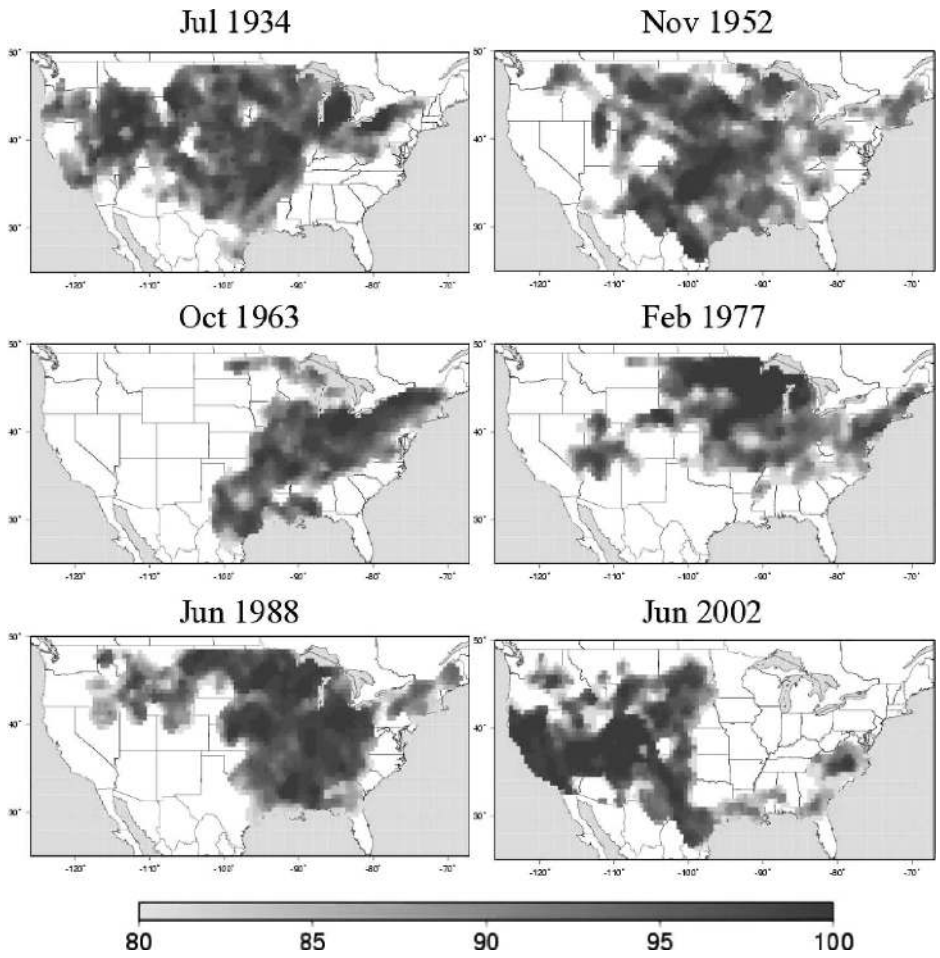

FIG. 2. Maps of spatial patterns of the most severe agricultural droughts identified. Each map shows drought severity (derived from soil moisture) for a specific month.

eth century. The maps also verify that the 1960s, late 1970s, and early 2000s droughts had a large spatial extent as well, with the early 2000s drought having a much larger impact on the western United States.

Figure 3 shows the percentage of area characterized as being in agricultural (soil moisture) drought, in the western, eastern, central, and continental United States. Also shown on the same figure are the soil moisture percentiles averaged over the respective areas. The 2000s drought stands out as the prominent feature of the time series for the West. The 1930s and late-1980s droughts also appear as severe events, with the late-1980s drought being as severe as that of the 1930s, but at a smaller spatial extent. The 1977 drought appears as a major event, in agreement with past studies (Keyantash and Dracup 2004). The 1930s and 1950s droughts have the largest spatial extent for the central United States, with the latter event being the most severe. An interesting feature of the eastern U.S. soil moisture time series is the large month-to-month vari-

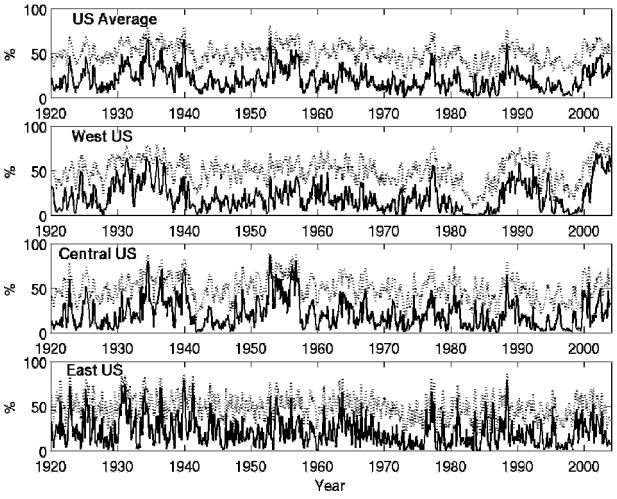

FIG. 3. Monthly time series of percent area (black line) characterized as agricultural drought, and spatially averaged drought severity (derived from soil moisture; gray line). The subplots correspond to the entire, western, central, and eastern United States, respectively.

Unauthenticated | Downloaded 08/22/22 08:12 PM UTC

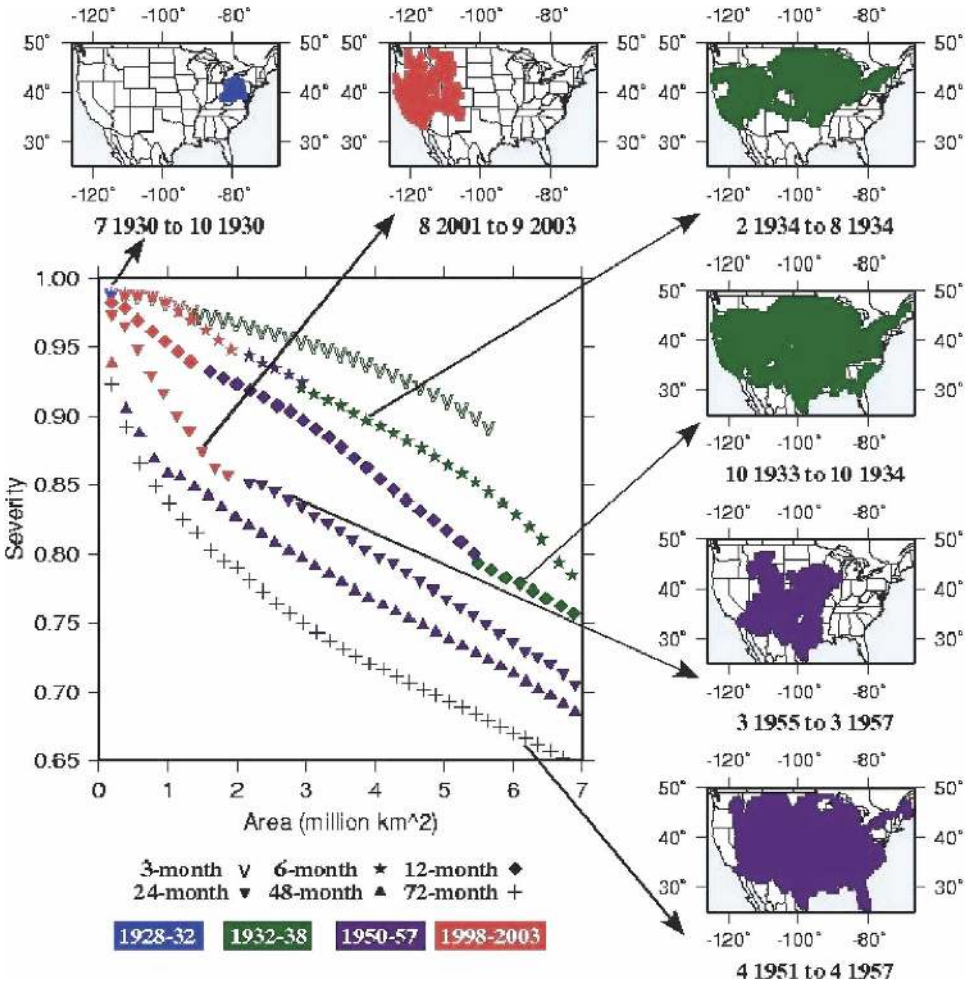

FIG. 4. SAD envelope curves based on soil moisture. Each curve corresponds to a specific drought duration (3, 6, 12, 24, 48, and 72 months). Different colors correspond to the drought events from which the specific point was derived.

ability, indicating that dry (and wet) spells in this region are much less persistent both temporally and spatially than in the central and western United States.

The envelope curve was constructed by first finding the maximum severity for each predefined duration at area increments of 100 pixels from the SAD curves of all of the drought events that are identified. Each point in the envelope curve was then associated with the event from which it was derived. Figure 4 shows the envelope curve of agricultural droughts (based on soil moisture) for selected event durations, along with maps of the cells over which severity was averaged to produce selected points on the curves. The results were similar for the durations that are not shown on the figure. The 3-month envelope curve is mostly dominated by the 1930s drought, with the early 2000s drought appearing for relatively small areas. The early 2000s drought is also most severe when averaged over small areas (up to 2×10^6 km^2, or about 24% of the total area of the conterminous United States) for the 6-, 12- and 24-month durations. It is interesting to note that this event ranks as the most severe drought when averaged over areas up to 2×10^6 km^2, covering almost the entire western United States, for a 2-yr duration (2001–03). The 1930s drought dominates the larger spatial extents of the 3- and 6-month duration curves, but it only appears on the 12-month curve when averaged over very large areas (larger than 5.5 million km^2). Based on our simulations, the 1950s drought appears to be the most severe at an increasing number of area values as durations become longer, especially for 1-yr durations and longer. In particular, the 1950s drought is the most severe for the 12- and 24-month durations, and for areas ranging from 1.5 to almost 7 million km^2

Unauthenticated | Downloaded 08/22/22 08:12 PM UTC

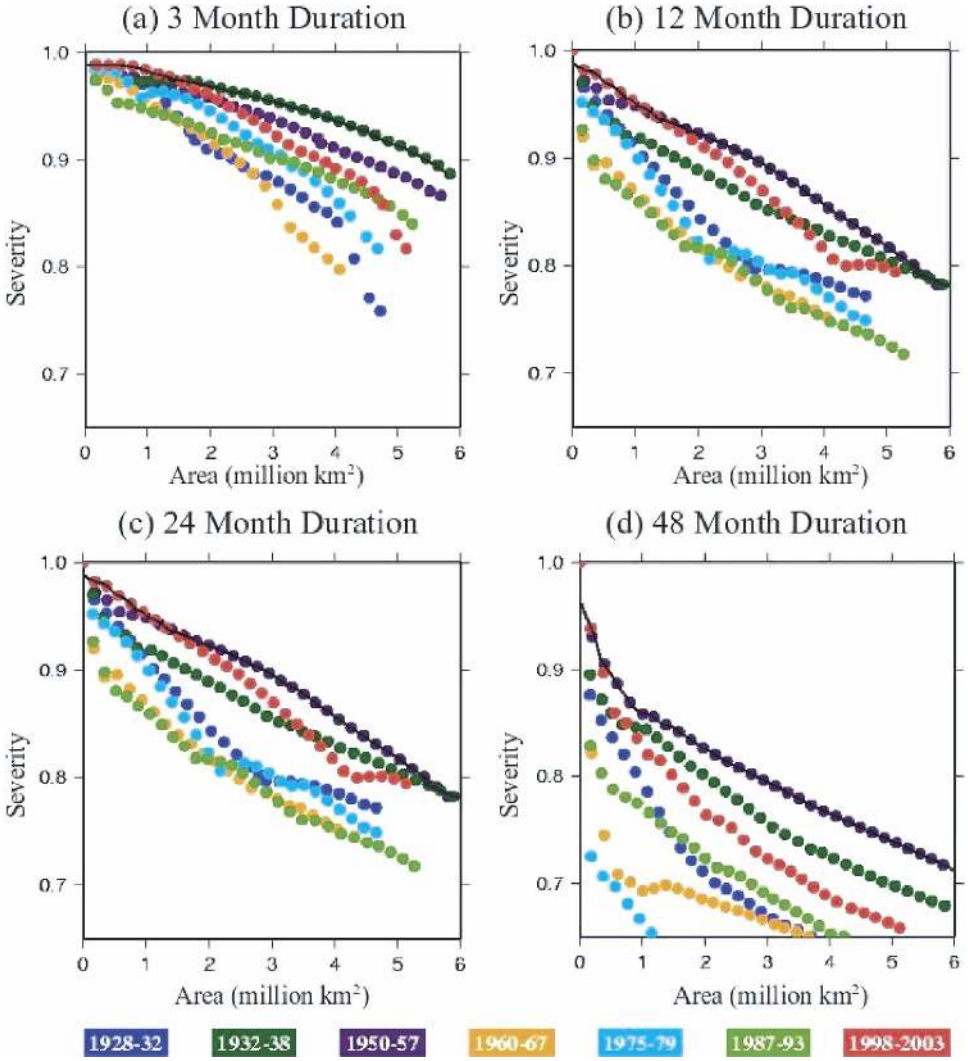

FIG. 5. SAD curves for the major drought events identified from soil moisture. Each subplot corresponds to different analysis duration: (a) 3, (b) 12, (c) 24, and (d) 48 months.

(about 20%–90% of the continental United States). The 1950s drought is most severe at all areas for the 48- and 72-month envelope curves.

More insight into the characteristics of individual droughts may be gained by examining their SAD curves for different durations. For the 3-month duration (Fig. 5a), we can see that the 1930s, 1950s, late 1970s, and early 2000s droughts are very close, in terms of severity, for areas up to about 2 million km^2. As the areas increase, however, the 1930s drought dominates. For areas larger than about 3 million km^2, the 1930s drought is much more intense than the 1950s drought. In the 12-month SAD curves (Fig. 5b), the 1950s drought dominates for most of the area values, with the exception of the smaller spatial extents where the early 2000s drought ranked as the worst 1-yr drought. The same result appears on the 2-yr SAD curves (Fig. 5c). The early 2000s and the 1950s droughts are much more severe than the others. Note that at areas higher than 2 million km^2, the early 2000s drought curve shows a steep decrease in slope. This is because about half of the area corresponding to this drought experienced a recovery during the 2-yr period (of the SAD curve) and, hence, the average severity is much lower compared to that averaged over a smaller area that remained in drought conditions for most of the 2-yr period. Notice that the 1988 drought shows severe conditions even for the largest areas (Figs. 5a, 5b, and 5c); however, because its severity is much smaller than that of the other major events, the 1988 drought does not appear on the envelope curve. Figure 5d shows SAD curves for the 4-yr duration. The 1950s drought, in this

Unauthenticated | Downloaded 08/22/22 08:12 PM UTC

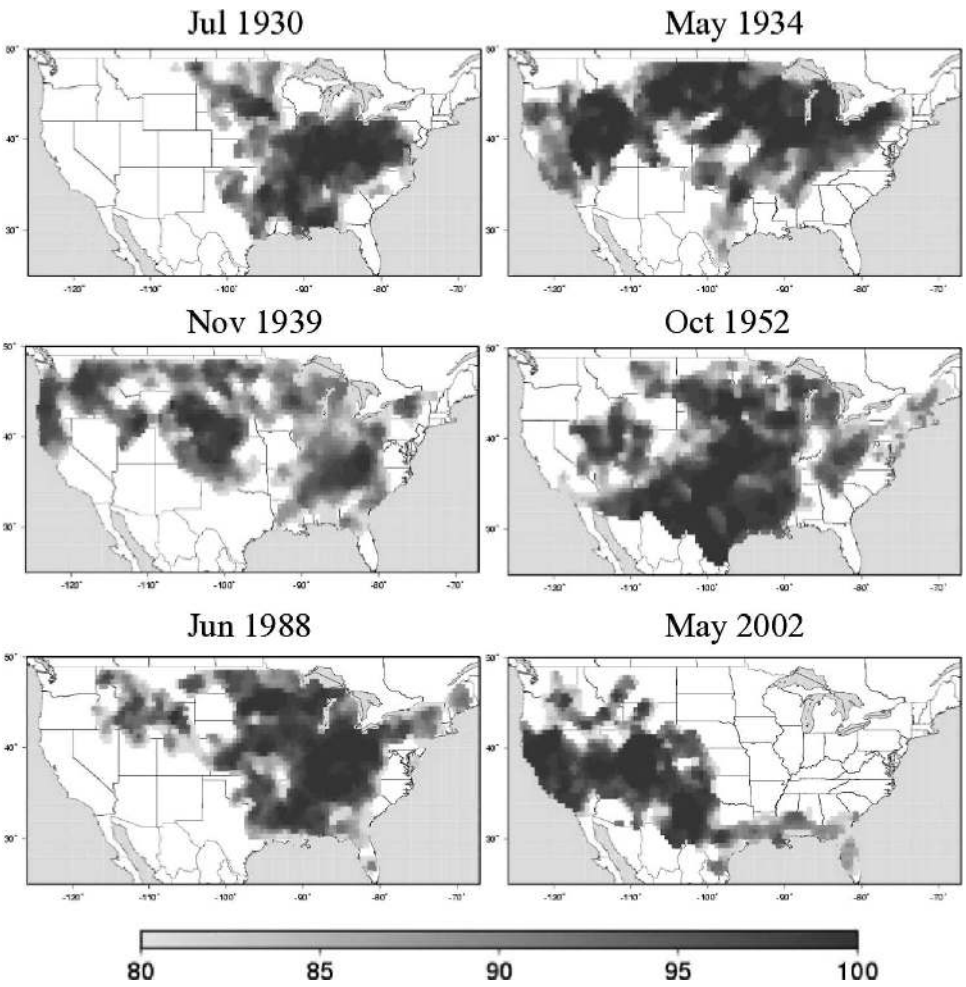

FIG. 6. Maps of spatial patterns of the most severe hydrological droughts identified. Each map shows drought severity (derived from runoff) for a specific month.

case, is much more severe than the other major drought events.

From the short-duration figures, we would expect the 1930s drought to be more severe than the 1950s drought, at least when averaged over the largest areas. Nonetheless, because our analysis technique prevented the 1930s drought from continuing during 1932, as a result of a 1-month recovery and subsequent relocation, the drought was split into two events—one in 1928–32 and one in 1932–38. The effect of this is most evident in the longest duration results, as is shown in Fig. 5.

b. Runoff droughts

The number of drought events that are identified based on streamflow data (251) was similar to that based on soil moisture data. Two events lasted for a continuous period of 72 months; not surprisingly, these were the 1930s and 1950s droughts (1932–38 and 1950–57). Hydrologic droughts with durations longer than 4 yr also included events during 1928–32, 1987–91, and 1999–2003. In terms of spatial extent, the largest droughts were 1932–38, 1950–57, 1999–2003, 1987–91, 1928–32, 1938–41, and 1975–78, in order of decreasing area. The major events that are identified using runoff percentiles are essentially the same as those identified from the soil moisture–based analysis. It is interesting to note, though, that the 1930s drought is split into three distinct events, while the 1950s drought again is identified as a single continuous event. Figure 6 shows spatial maps of each of the major runoff-derived droughts for a specific month. The displayed month was selected using the same approach as in Fig. 2. The maps show that the "Dust Bowl" had the largest impact, in terms of streamflow, in the mid-1930s. The 1950s drought had a very large spatial extent, covering the Great Plains and reaching southward to Texas and parts of Colorado. Finally, the 1988 and early 2000s

Unauthenticated | Downloaded 08/22/22 08:12 PM UTC

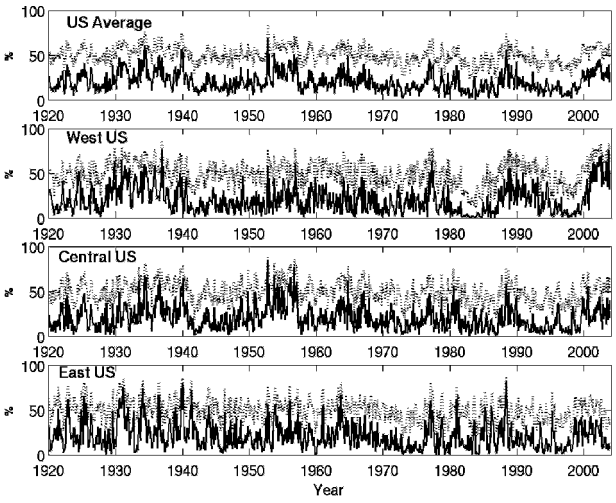

FIG. 7. Monthly time series of percent area (black line) characterized as hydrological drought, and spatially averaged drought severity (derived from runoff; gray line). The subplots correspond to the entire, western, central, and eastern United States, respectively.

drought spatial patterns agree well with the ones derived from soil moisture.

The temporal variations of hydrological drought area over the continental United States and areally averaged runoff percentiles are shown in Fig. 7. The trends in the time series of runoff appear to be similar to the ones for soil moisture. However, the magnitude of the 1930s and 1950s droughts, in terms of runoff, appears to be less pronounced than that for the soil moisture analysis. Another difference with the soil moisture time series is that the month-to-month variability is much larger, which is in agreement with the memory associated with the processes governing soil moisture variability. Nonetheless, the drought events that appear to be the most severe are the same as those identified from soil moisture.

The envelope curve is rather different from the soil moisture envelope curve. Figure 8 shows the runoff-based envelope curve for selected durations and area increments up to 7 million km^2. The prominent feature of the curve is that the early 2000s drought occupies a larger portion of the 3- to 24-month curves than in the soil moisture analysis. As we can see in the accompanying spatial maps, the early 2000s drought effectively covers the entire western United States, and is the most severe drought of record for durations up to 2 yr. This suggests that there were minimal recovery periods for the entire region, amplifying its severity. The 1930s drought stands out as the most severe drought for the mid- to larger spatial extents with decreasing frequency from the 3-month- to the 1-yr-duration curves. The 1950s drought is the most severe event for the largest spatial extents and longest duration curves. In fact, it is always the most severe drought for areas larger than 2.5 million km^2 (30% of the continental United States), and for 24-, 48-month durations. Moreover, the 72-month envelope curve is occupied exclusively by the 1950s drought. For the smallest areas, the 1975–78 drought in the Great Lakes region occupies the leftmost part of the 3-month curve.

Figure 9 shows the SAD curves for these events for durations of 3, 12, 24, and 48 months. In the 3-month curves (Fig. 9a), the 1932–38, 1975–78, and 1999–2003 droughts plot close for small to midsize areas, with the latter two events displaying an expected decrease in severity for larger areas where the 1930s drought dominates. In Fig. 9b (12-month duration), the early 2000s drought dominates for areas up to 3 million km^2, with the 1950s drought having a similar (and eventually larger) severity as area increases. The 1932–38 drought appears as the last point on the envelope curve, but had a much smaller relative severity for smaller areas. This is also the case for the other 1930s drought (1928–32), which has a convex shape. This is an effect of the SAD technique; that is, the contiguity constraint forces the algorithm to search for the largest severity pixels in the neighborhood of the area that is already computed. Therefore, for some of the smaller areas the average severity is smaller than the average severity of the larger areas. In the 24-month SAD curves (Fig. 9c), the early 2000s drought is clearly dominant for small spatial extents, but for mid- to larger areas, the 1950s drought occupies the envelope curve, although it has a similar severity than the 1930s drought events. The 48-month SAD curves (Fig. 9d) show that the 1950s drought is the most severe drought, with the exception of the very small areas that show the early 2000s drought as the one having the largest severity.

8. Discussion

Table 1 lists the major droughts in the twentieth century, as identified in the literature, using a variety of methods. In this section, we evaluate our results in comparison with the other studies summarized in Table 1. All of the events shown in Table 1 were also identified in our analysis. An interesting comparison can be made with the results from Cook et al. (1999), who used tree-ring chronologies to reconstruct U.S. droughts from 1700 to 1978, using monthly PDSI. They used principal component analysis to identify climate regions and then examined the average signal over the United States for severe drought events. They found that the 1930s Dust Bowl was the most severe drought in the continental

Unauthenticated | Downloaded 08/22/22 08:12 PM UTC

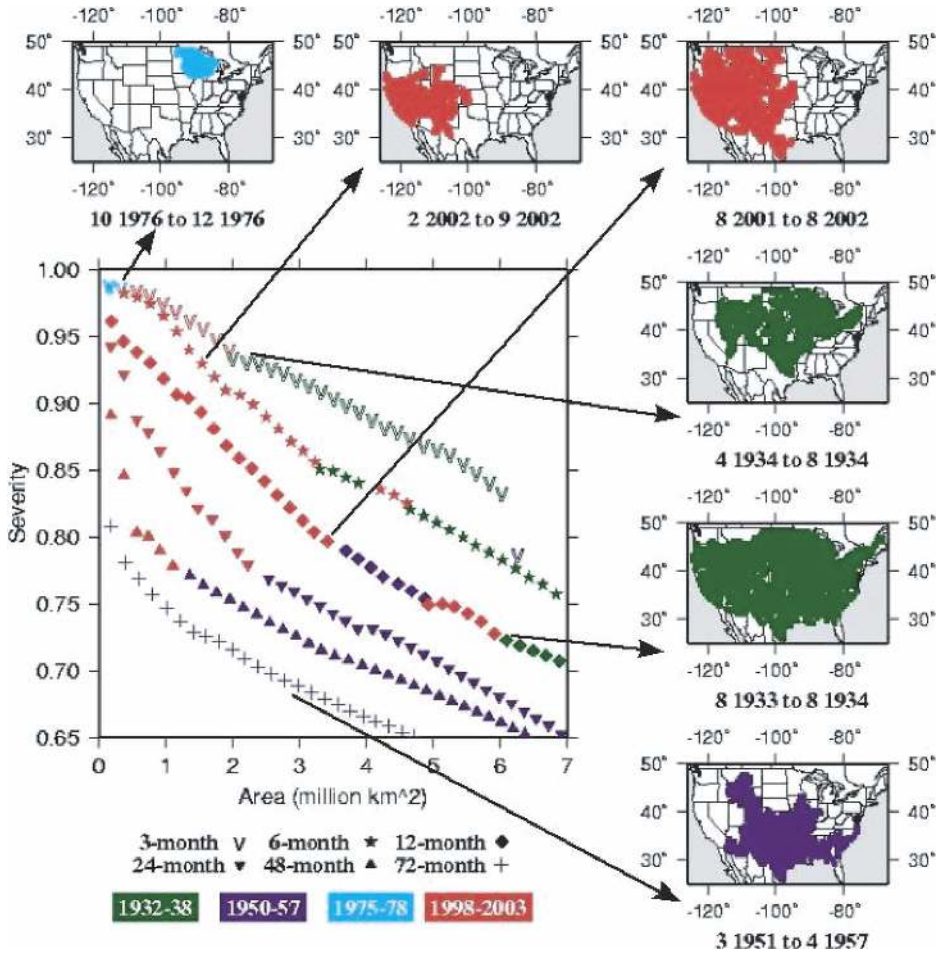

FIG. 8. SAD envelope curves based on runoff. Each curve corresponds to a specific drought duration (3, 6, 12, 24, 48, and 72 months). Different colors correspond to the drought events from which the specific point was derived.

United States during their period of analysis (1700–1978). They also found that the third most severe drought occurred in 1977, which qualitatively agrees with our results, which show that the mid- to late 70s drought is the most severe hydrological drought for small spatial extents. Although the 1950s drought was found as a notable drought event by Cook et al. (1999), it did not have the same magnitude as shown in our analysis. Nevertheless, in terms of the temporal resolution of the Cook et al. study (monthly) our results seem to be in accordance, in particular, our finding that the 1930s had the most intense drought period (high severity for short durations), on average, in the United States.

Conceptually, the sequence of drought types begins with meteorological drought, and, as its duration increases, agricultural (soil moisture) and hydrologic (streamflow) drought follow. Simplistically, one would expect that the most severe droughts for runoff should be about the same as for soil moisture, especially taking into account the time scales of our analysis. However, our results showed that although the early 2000s drought had a relatively high soil moisture–based severity, it occupied a much larger portion of the runoff-based envelope curve. It is worth exploring the causes of this difference, especially when taking into account the socioeconomic importance of the early 2000s western U.S. drought.

The SAD curves are constructed based on the average cumulative severity of different areas that are experiencing drought over a given duration. Runoff is affected by soil moisture deficits; if we examine the spatially averaged correlation coefficient between soil moisture and runoff for the periods of the three major drought events (1930s, 1950s, and early 2000s), we find that the correlation is much higher for the early 2000s drought (Table 2). A possible explanation might be inferred from the correlations between soil moisture and

Unauthenticated | Downloaded 08/22/22 08:12 PM UTC

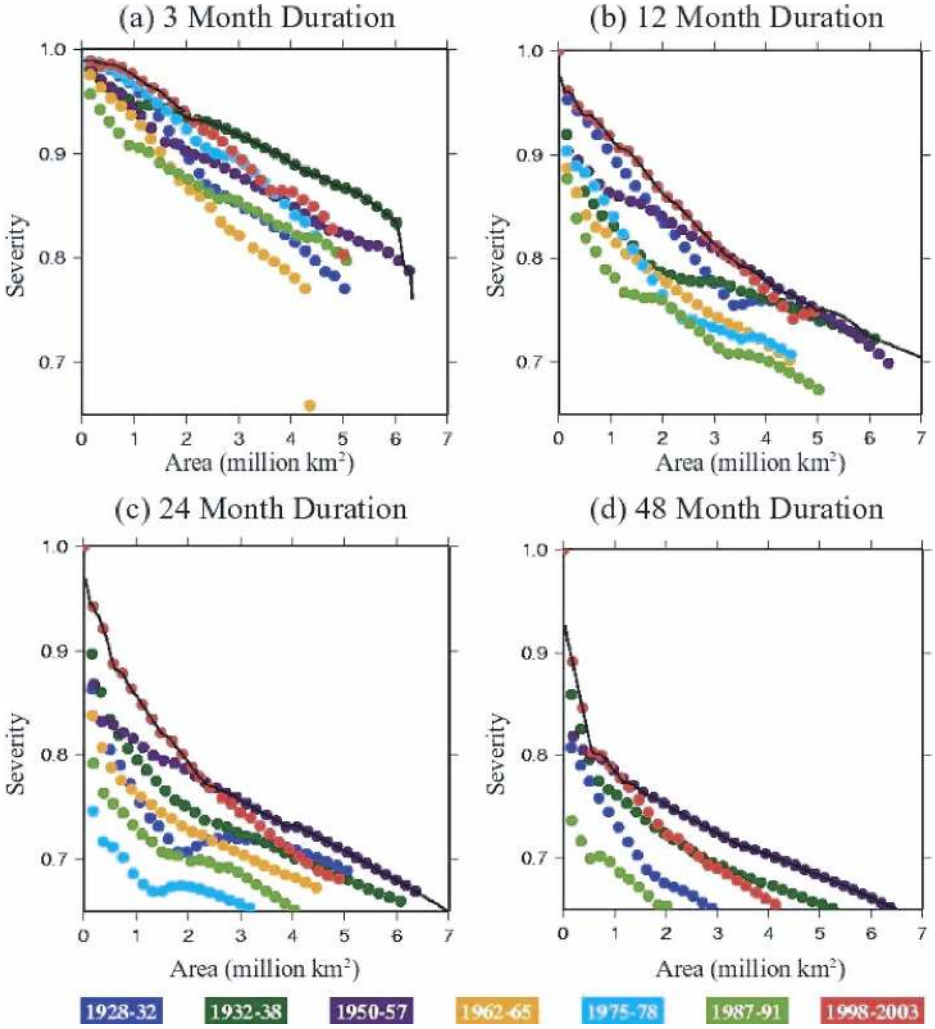

FIG. 9. SAD curves for the major drought events identified from runoff. Each subplot corresponds to different analysis duration: (a) 3, (b) 12, (c) 24, and (d) 48 months.

runoff with precipitation, in the context of drought recovery. Table 2 shows the correlations between the spatially averaged (over the western United States) soil moisture, runoff, and precipitation percentiles. Precipitation has a much higher correlation with runoff than with soil moisture. This follows from the fact that soil moisture is relatively more persistent than runoff, and that the latter responds more quickly to precipitation signals. The early 2000s hydrological drought is more severe (when compared to the relative position of the respective agricultural drought on the SAD envelope curve), mainly for the 6- and 12-month durations and areas that occupy the middle part of the curves. Figure 10 shows the autocorrelation of the spatially averaged monthly precipitation for the three drought events and lags from 1 to 12 months. The autocorrelation is significantly higher for the early 2000s drought, which suggests that dry (or wet) spells during that drought event were longer than during the other two droughts. Because runoff responds faster to precipitation, parts of the areas under hydrological drought in the 1930s and 1950s recovered, thus, decreasing the average severity.

The above discussion simply describes the processes that drive drought events of large magnitude. An increasing number of studies have looked at the relationship between extreme droughts and climate teleconnections, such as ENSO and the PDO (e.g., Trenberth et al. 1988; Schubert et al. 2004). A simple correlation analysis between the VIC-simulated end-of-summer soil moisture and runoff, and January SST anomalies (not shown here) exhibits strong correlations in the northwestern and southwestern United States, as expected. However, a similar analysis of end-of-summer soil moisture and runoff for individual persistent severe

Unauthenticated | Downloaded 08/22/22 08:12 PM UTC

TABLE 1. Notable twentieth-century droughts in the conterminous United States.

Dates	Location	Type of data	Sources
1910–13	Western Kansas	PDSI	Palmer (1965); Ludlum (1982)
1931–40	Great Plains eastward to Great Lakes, Southwestern United States	Precipitation, temperature; reconstructed PDSI	Schubert et al. (2004); Cook et al. (1999); Weakly (1965), as cited in Bark (1978); Ludlum (1982)
1947	Central Iowa	PDSI	Palmer (1965)
Mid-1950s	Great Plains to southeastern United States	Reconstructed PDSI	Cook et al. (1999); Stahle and Cleaveland (1988); Palmer (1965); Weakly (1965), as cited in Bark (1978); Ludlum (1982); Karl and Quayle (1981)
1961–66	Northeastern United States, North Dakota	PDSI, reconstructed PDSI	Cook and Jacoby (1977); Cook et al. (1999); Palmer (1965); Ludlum (1982)
Mid-1970s	Western United States	PDSI, aggregate drought index	Felch (1978); Webb et al. (2004), citing NOAA (2004); Ludlum (1982); Keyantash and Dracup (2004)
1980–81	Southern and southeastern United States	PDSI, *Z*-index, population-weighted cooling degree-days as related to electrical energy sales	Karl and Quayle (1981)
1987–88	West coast, northwestern United States, north-central United States, Great Plains, UT	Precipitation, PDSI, aggregate drought index	Trenberth et al. (1988); Webb et al. (2004), citing NOAA (2004); Atlas et al. (1993); Keyantash and Dracup (2004)
1996	Utah	PDSI	Webb et al. (2004), citing NOAA (2004)

drought events did not display any characteristic spatial structure, suggesting that a more complicated climate signal is associated with these extreme droughts (Hoerling and Kumar 2003).

9. Summary and conclusions

Retrospective simulations of soil moisture and runoff across the continental United States were performed for the period of 1920–2003. An empirical probability distribution was fit to these data to produce percentiles corresponding to the monthly soil moisture and runoff for each half-degree grid cell. Contiguous grid cells experiencing lower than 20th percentile soil moisture, or streamflow, at each monthly time step were considered to constitute drought events. These events were then reclassified based on their temporal continuity. Grid cells included in the final drought classification were then input to a scheme termed the severity–area–duration analysis, which represents the relationship between these drought characteristics for each drought event. Envelope curves for each drought duration were then produced, representing the most severe drought events in the study period over the study domain.

Drought severity that is calculated using the simu-

TABLE 2. Correlations between spatially averaged (over the western United States) precipitation, soil moisture, and runoff percentiles for three different drought events (1930s, 1950s, and 2000s).

	Correlation coefficient R^2		
Drought event	Runoff–soil moisture	Precipitation–runoff	Precipitation–soil moisture
1930s	0.686	0.655	0.232
1950s	0.766	0.759	0.357
2000s	0.922	0.799	0.570

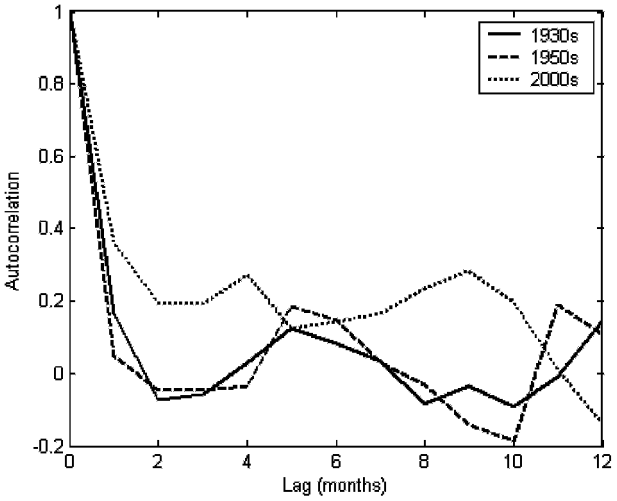

FIG. 10. Autocorrelation coefficient of the spatially averaged (over the western United States) precipitation for three different periods corresponding to three drought events (1930s, 1950s, and 2000s). Values of the autocorrelation coefficient up to a lag of 12 months are shown.

Unauthenticated | Downloaded 08/22/22 08:12 PM UTC

lated soil moisture and runoff percentiles is limited by errors and biases inherent in the model physics, parameters, and forcing data. Nonetheless, validation of VIC soil moisture and streamflow predictions in different regions of the United States, and the identification of drought events that have already been cited as extreme droughts in the twentieth century, support our use of an approach based on soil moisture and runoff that are derived from VIC model simulations. The model products provide a spatially and temporally continuous dataset of hydrologic variables, which are estimated using a physically based model that accounts for various land surface processes (such as cold land processes), in contrast with other drought indices that employ simple water balance models. The technique that is presented in this paper employs a physically based criterion for drought identification that is applicable across climate regions. Because many of the most severe droughts in the United States cross climate region boundaries, regionalization that other studies have employed limits the maximum spatial component of drought impacts—a limitation that our method avoids. Whereas many studies produce time series of regional drought evolution, SAD analysis directly characterizes specific drought events, both spatially and temporally. SAD is, thus, meant to be a supplementary tool in drought characterization.

The primary features of the evolution of twentieth-century U.S. droughts, as reflected in the constructed SAD and envelope curves, can be summarized as follows:

- The drought events of the 1930s and 1950s were the most severe experienced in the (last 80 yr of the) twentieth century for large areas. However, in our analysis the 1930s Dust Bowl was the most intense drought (largest severity for short durations), a conclusion that agrees with previous studies that examined drought severity over short time scales. On the other hand, the 1950s drought was the most persistent event, having the largest severity for long durations.
- The early 2000s drought in the western United States is among the most severe in the period of record, especially when averaged over small areas and short durations. Because the early 2000s drought is still developing, it is possible that it may appear among the most severe droughts at longer durations.
- In general, the most severe agricultural droughts (defined by simulated soil moisture) were also among the most severe hydrologic droughts (defined by simulated runoff). The early 2000s drought, however, occupies a larger portion of the hydrologic drought envelope curve than does its agricultural companion.
- Runoff tends to recover in response to precipitation more quickly than soil moisture, so the severity of hydrologic drought during the 1930s and 1950s was dampened by short wet spells, while the severity of the early 2000s drought remained high because of the relative absence of these short-term phenomena.

In theory, SAD curves can be treated similarly to DAD curves, in terms of water management. The primary purpose of this type of characterization is to provide a historical perspective when planning for future drought mitigation. However, because of model uncertainty, this technique should only be used in conjunction with existing drought-planning tools. SAD could also be applied in the context of climate change analysis to assess whether climate trends are changing (or have the potential to alter) the severity of drought occurrence. An interesting application of this technique would be the coupling of a general circulation model (GCM) with a land surface scheme (e.g., VIC) to provide the input dataset to the SAD technique. In a hydrologic-forecasting context, ensemble techniques could be incorporated and corresponding probabilities of drought occurrence can be estimated. Future studies may include real-time applications of this technique across the continental United States with an emphasis on the probability of recovery.

REFERENCES

Abdulla, F. A., D. P. Lettenmaier, E. F. Wood, and J. A. Smith, 1996: Application of a macroscale hydrologic model to estimate the water balance of the Arkansas-Red River basin. *J. Geophys. Res.,* **101,** 7449–7460.

Alley, W. M., 1984: The Palmer Drought Severity Index: Limitations and assumptions. *J. Climate Appl. Meteor.,* **23,** 1100–1109.

Atlas, R., N. Wolfson, and J. Terry, 1993: The effect of SST and soil moisture anomalies on GLA model simulations of the 1988 U.S. summer drought. *J. Climate,* **6,** 2034–2048.

Bark, L. D., 1978: History of American drought. *North American Droughts*, N. J. Rosenberg, Ed., Westview Press, 9–23.

Byun, H., and D. A. Wilhite, 1999: Objective quantification of drought severity and duration. *J. Climate,* **12,** 2747–2756.

Cherkauer, K. A., and D. P. Lettenmaier, 2003: Simulation of spatial variability in snow and frozen soil. *J. Geophys. Res.,* **108,** 8858, doi:10.1029/2003JD003575.

Climate Prediction Center, cited 2005: U.S. soil moisture monitoring. National Weather Service. [Available online at http://www.cpc.ncep.noaa.gov/soilmst/.]

Cook, E. R., and G. C. Jacoby Jr., 1977: Tree-ring-drought relationships in the Hudson Valley, New York. *Science,* **198,** 399–401.

——, D. M. Meko, D. W. Stahle, and M. K. Cleaveland, 1999: Drought reconstructions for the continental United States. *J. Climate,* **12,** 1145–1162.

Unauthenticated | Downloaded 08/22/22 08:12 PM UTC

Cosgrove, B. A., and Coauthors, 2003: Land surface spin-up behavior in the North American Land Data Assimilation System (NLDAS). *J. Geophys. Res.,* **108,** 8845, doi:10.1029/2002JD003316.

Dai, A., K. E. Trenberth, and T. R. Karl, 1998: Global variations in droughts and wet spells. *Geophys. Res. Lett.,* **25,** 3367–3370.

——, ——, and T. Qian, 2004: A global data set of Palmer Drought Severity Index for 1870–2002: Relationship with soil moisture and effects of surface warming. *J. Hydrometeor.,* **5,** 1117–1130.

Dalezios, N. R., A. Loukas, L. Vasiliades, and E. Liakopoulos, 2000: Severity-duration-frequency analysis of droughts and wet periods in Greece. *Hydrol. Sci.,* **45,** 751–769.

Daly, C., R. P. Neilson, and D. L. Phillips, 1994: A statistical-topographic model for mapping climatological precipitation over mountainous terrain. *J. Appl. Meteor.,* **33,** 140–158.

Dhar, O. N., and S. Nandargi, 1993: Envelope depth-area-duration rain depths for different homogeneous rainstorm zones of the Indian region. *Theor. Appl. Climatol.,* **47,** 117–125.

Dracup, J. A., K. S. Lee, and E. G. Paulson Jr., 1980a: On the definition of droughts. *Water Resour. Res.,* **16,** 297–302.

——, ——, and ——, 1980b: On the statistical characteristics of drought events. *Water Resour. Res.,* **16,** 289–296.

Federal Emergency Management Agency, 1995: National mitigation strategy: Partnerships for building safer communities. FEMA Mitigation Directorate, 40 pp.

Felch, R. E., 1978: Drought: Characteristics and assessment. *North American Droughts,* N. J. Rosenberg, Ed., AAAS Selected Symposia, Vol. 15, Westview Press, 25–42.

Grebner, D., and T. Roesch, 1997: Regional dependence and application of DAD relationships. *Proc. FRIEND '97—Regional Hydrology: Concepts and Models for Sustainable Water Resource Management,* Postojna, Slovenia, IAHS, IAHS Publication 246, 223–230.

Hamlet, A. F., and D. P. Lettenmaier, 2005: Production of temporally consistent gridded precipitation and temperature fields for the continental United States. *J. Hydrometeor.,* **6,** 330–336.

Hisdal, H., and L. M. Tallaksen, 2003: Estimation of regional meteorological and hydrological drought characteristics: A case study for Denmark. *J. Hydrol.,* **281,** 230–247.

Hoerling, M., and A. Kumar, 2003: The perfect ocean for drought. *Science,* **299,** 691–694.

Huang, J., H. M. Van den Dool, and K. P. Georgakakos, 1996: Analysis of model-calculated soil moisture over the United States (1931–1993) and applications to long-range temperature forecasts. *J. Climate,* **9,** 1350–1362.

Karl, T. R., and R. G. Quayle, 1981: The 1980 summer heat wave and drought in historical perspective. *Mon. Wea. Rev.,* **109,** 2055–2073.

——, and A. J. Koscielny, 1982: Drought in the United States: 1895-1981. *J. Climatol.,* **2,** 313–329.

——, C. N. Williams Jr., F. T. Quinlan, and T. A. Boden, 1990: United States Historical Climatology Network (HCN) serial temperature and precipitation data. Carbon Dioxide Information and Analysis Center, Oak Ridge National Laboratory Environmental Science Division Publication No. 3404, 389 pp.

Keyantash, J. A., and J. A. Dracup, 2004: An aggregate drought index: Assessing drought severity based on fluctuations in the hydrologic cycle and surface water storage. *Water Resour. Res.,* **40,** W09304, doi:10.1029/2003WR002610.

Liang, X., D. P. Lettenmaier, E. F. Wood, and S. J. Burges, 1994: A simple hydrologically based model of land surface water and energy fluxes for GSMs. *J. Geophys. Res.,* **99,** 14 415–14 428.

——, ——, ——, and ——, 1996: One-dimensional statistical dynamic representation of subgrid spatial variability of precipitation in the two-layer variable infiltration capacity model. *J. Geophys. Res.,* **101,** 21 403–21 422.

Lohmann, D., E. Raschke, B. Nijssen, and D. P. Lettenmaier, 1998: Regional scale hydrology; II, Application of the VIC-2L model to the Weser River, Germany. *Hydrol. Sci. J.,* **43,** 143–158.

Ludlum, D. M., 1982: *The American Weather Book*. Houghton-Mifflin, 296 pp.

Maurer, E. P., A. W. Wood, J. C. Adam, and D. P. Lettenmaier, 2002: A long-term hydrologically based dataset of land surface fluxes and states for the conterminous United States. *J. Climate,* **15,** 3237–3251.

Mekis, E., and W. D. Hogg, 1999: Rehabilitation and analysis of Canadian daily precipitation time series. *Atmos.–Ocean,* **37,** 53–85.

Mitchell, K. E., and Coauthors, 2004: The multi-institution North American Land Data Assimilation System (NLDAS): Utilizing multiple GCIP products and partners in a continental distributed hydrological modeling system. *J. Geophys. Res.,* **109,** D07S90, doi:10.1029/2003JD003823.

National Climatic Data Center, cited 2003: Coop summary of the day—CDMP—Pre 1948, Data documentation for data set 3206 (DSI-3206), 18 pp. [Available online at http://www4.ncdc.noaa.gov/ol/documentlibrary/datasets.html.]

Nijssen, B., D. P. Lettenmaier, X. Liang, S. W. Wetzel, and E. F. Wood, 1997: Streamflow simulation for continental-scale river basins. *Water Resour. Res.,* **33,** 711–724.

——, R. Schnur, and D. P. Lettenmaier, 2001: Global retrospective estimation of soil moisture using the Variable Infiltration Capacity land surface model, 1980–93. *J. Climate,* **14,** 1790–1808.

Oladipo, E. O., 1986: Spatial patterns of drought in the Interior Plains of North America. *J. Climatol.,* **6,** 495–513.

Palmer, W. C., 1965: Meteorological drought. U.S. Department of Commerce, Weather Bureau Res. Paper 45, 58 pp.

Robock, A., K. Y. Vinnikov, G. Srinivasan, J. K. Entin, S. E. Hollinger, N. A. Speranskaya, S. Liu, and A. Namkhai, 2000: The Global Soil Moisture Data Bank. *Bull. Amer. Meteor. Soc.,* **81,** 1281–1299.

——, and Coauthors, 2003: Evaluation of the North American Land Data Assimilation System over the southern Great Plains during the warm season. *J. Geophys. Res.,* **108,** 8846, doi:10.1029/2002JD003245.

Schubert, S. D., M. J. Suarez, P. J. Pegion, R. D. Koster, and J. T. Bacmeister, 2004: On the cause of the 1930s Dust Bowl. *Science,* **303,** 1855–1859.

Sheffield, J., G. Goteti, F. Wen, and E. F. Wood, 2004: A simulated soil moisture based drought analysis for the USA. *J. Geophys. Res.,* **109,** D24108, doi:10.1029/2004JD005182.

Soulé, P. R., 1993: Hydrologic drought in the contiguous United States, 1900-1989: Spatial patterns and multiple comparison of means. *Geophys. Res. Lett.,* **20,** 2367–2370.

Stahle, D. W., and M. K. Cleaveland, 1988: Texas drought history

Unauthenticated | Downloaded 08/22/22 08:12 PM UTC

reconstructed and analyzed from 1698 to 1980. *J. Climate,* **1,** 69–74.

Trenberth, K. E., G. W. Branstator, and P. A. Arkin, 1988: Origins of the 1988 North American drought. *Science,* **242,** 1640–1645.

U.S. Drought Monitor, cited 2003: Drought monitor: State-of-the-art blend of science and subjectivity. National Drought Mitigation Center. [Available online at http://drought.unl.edu/dm/archive/99/classify.htm.]

Vincent, L. A., and D. W. Gullett, 1999: Canadian historical and homogeneous temperature datasets for climate change analyses. *Int. J. Climatol.,* **19,** 1375–1388.

Weakly, H. E., 1965: Recurrence of drought in the Great Plains during the last 700 years. *Agric. Eng.,* **46,** 85.

Webb, R. H., G. J. McCabe, R. Hereford, and C. Wilkowske, 2004: Climate fluctuations, drought, and flow in the Colorado River. USGS Fact Sheet 3062-04, 4 pp.

Wilhite, D. A., and M. H. Glantz, 1985: Understanding the drought phenomenon: The role of definitions. *Water Int.,* **10,** 111–120.

Willeke, G., J. R. M. Hosking, J. R. Wallis, and N. B. Guttman, 1994: *The National Drought Atlas*. Institute for Water Resources Rep. 94-NDS-4, 587 pp.

Wood, E. F., D. P. Lettenmaier, X. Liang, B. Nijssen, and S. W. Wetzel, 1997: Hydrological modeling of continental-scale basins. *Annu. Rev. Earth Planet. Sci.,* **25,** 279–300.

World Meteorological Organization, 1969: Manual for depth-area-duration analysis of storm precipitation. WMO Rep. 237.TP.129, 114 pp.

Unauthenticated | Downloaded 08/22/22 08:12 PM UTC